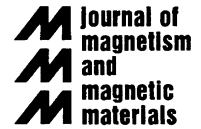




ELSEVIER

Journal of Magnetism and Magnetic Materials 248 (2002) 418–422



www.elsevier.com/locate/jmmm

# An investigation of time-dependent domain wall pinning effects in Tb/Fe multilayer thin films

G.N. Phillips<sup>a,\*</sup>, K. O'Grady<sup>b</sup>, M. El-Hilo<sup>c</sup>

<sup>a</sup>Information Storage Technology Group, MESA<sup>+</sup> Research Institute, University of Twente, 7500 AE Enschede, The Netherlands

<sup>b</sup>Magnetic Materials Research Group, Department of Physics, The University of York, Heslington, York, YO10 5DD, UK

<sup>c</sup>Department of Physics, University of Bahrain, P.O. Box 32038, Isa Town, Bahrain

Received 23 July 2001

## Abstract

Reverse domain nucleation time measurements have been performed on two Tb/Fe multilayer magneto-optic films exhibiting different degrees of domain wall pinning. A linear relationship between  $\ln$  (reverse domain nucleation time) and the applied field has been predicted and observed for a sample exhibiting weak domain wall pinning. This is in agreement with theoretical work presented which addresses time dependence in systems possessing weak domain wall pinning. A non-linear relationship applicable over a restricted field range has been derived for a sample exhibiting strong domain wall pinning. Experimental results have indicated that this relationship is also valid. © 2002 Elsevier Science B.V. All rights reserved.

**Keywords:** Multilayers; Magneto-optic recording media; Magnetization reversal; Magnetic viscosity

## 1. Introduction

Tb/Fe multilayer thin films have shown potential as a media for magneto-optic recording [1]. Magnetisation reversal in such films is usually described in terms of a well-established two-coercivity model whereby reverse domains nucleate and then grow [2]. Distinct energy barriers exist for reverse domain nucleation and domain wall motion which are, therefore, characterised by two separate coercive fields [3]. Domain growth via wall motion is governed by the strength of the

domain wall pinning exhibited by the film. Where weak domain wall pinning is prevalent reverse domains once nucleated will expand rapidly and magnetisation reversal will proceed swiftly. If strong domain wall pinning occurs, then reverse domain growth will be hindered and reversal will be less rapid.

Magneto-optic films generally exhibit a time dependency of magnetisation reversal, which is non-linear in  $\ln(t)$ , arising from thermal activation over local energy barriers that possess a narrow distribution [4–6]. Gaunt [7,8] has addressed such time-dependent magnetisation reversal for materials exhibiting weak and strong domain wall pinning, and also for single domain particles. Expressions were derived for the activation energy required to overcome weak and strong domain

\*Corresponding author. Present address: Philips Research, Prof. Holstlaan 4(WY21), 5656 AA Eindhoven, The Netherlands. Tel.: +31-40-27-44025; fax: +31-40-27-44927.

E-mail address: Gavin.Phillips@philips.com (G.N. Phillips).

wall pins, the associated activation volumes and their equivalent fluctuation fields. Gaunt defines weak domain wall pinning as the case when the wall breaks away co-operatively from many pinning sites at the coercive field. Similarly strong domain wall pinning is defined as when the wall breaks away from individual pins to sweep out a volume containing on average one more pin.

This paper uses the theoretical work of Gaunt as a basis to predict a linear relationship between  $\ln(t_n)$  and  $H$  is for magnetisation reversal via the nucleation and rapid expansion of reverse domains (due to weak domain wall pinning), where  $t_n$  is the time taken for a reverse domain to nucleate and become unpinned and  $H$  is the applied field. This relationship is confirmed experimentally at applied fields where weak domain wall pinning occurs. A non-linear relationship is predicted and observed over a restricted field range where strong domain wall pinning is prevalent.

## 2. Theory

Gaunt [7] addressed thermally induced magnetic viscosity in terms of energy barriers. The waiting time  $\tau$  before an energy barrier is overcome was given by

$$\tau^{-1} = f_0 \exp(-E_a/kT), \quad (1)$$

where  $E_a$  is the activation energy and  $kT$  is the Boltzmann energy.  $f_0$  is the spin precession frequency with a value between  $10^9$  and  $10^{12}$  Hz. The activation energy was considered to be the difference between the maximum and minimum energy positions of domain walls and for weak pinning was given by [7,8]

$$E_a = E_{\text{weak}}[1 - (H/H_0)], \quad (2)$$

where  $E_{\text{weak}}$  is a constant energy term dependent on the wall width and domain wall energy and  $H_0$  is the field required to unpin the wall without thermal activation. Magnetisation reversal in materials exhibiting weak pinning was assumed to proceed by domains becoming unpinned from many sites simultaneously in a co-operative process. Such reversal is the result of a breakdown in the Friedel steady-state model [8], which

describes reversal in materials exhibiting strong domain wall pinning. In this model, a domain wall on becoming unpinned is assumed to sweep out a volume that contains an average of one replacement pin. The activation energy for this process was given by [7,8]

$$E_a = E_{\text{strong}}[1 - (H/H_0)^{1/2}]^{3/2}, \quad (3)$$

where  $E_{\text{strong}}$  is proportional to the domain wall width and the maximum pinning force on the domain wall. From Eq. (1) it is possible to write

$$t_n/\tau = t_n f_0 \exp(-E_a/kT), \quad (4)$$

where  $t_n$  is the time taken for the magnetisation of a sample to reverse by a pre-defined amount, after the application of a field. The magnetisation of the sample is assumed to change via reverse domain nucleation and the unpinning of domain walls. If  $t_n/\tau \sim 1$  then  $E_a$  varies linearly with  $\ln(t_n)$  [7]:

$$E_a = kT \ln(t_n f_0). \quad (5)$$

Thus, by combining Eqs. (2) and (5) we obtain

$$\ln(t_n) = -\left(\frac{E_{\text{weak}}}{kTH_0}\right)H + \left[\frac{E_{\text{weak}}}{kT} - \ln(f_0)\right]. \quad (6)$$

Eq. (6) indicates that  $\ln(t_n)$  is a linear function of applied field where weak domain wall pinning prevails. It has been shown that the fluctuation field  $H_f = \Delta H/\Delta \ln(t)$  [9] and that  $H_f$  is inversely proportional to the activation volume  $v_a$  [7]. Thus, the slope of Eq. (6), i.e.  $\Delta \ln(t_n)/\Delta H$ , is proportional to  $v_a$ . This is consistent with Gaunt who stated that  $v_a$  is constant for weak domain wall pinning [7].

By combining Eqs. (3) and (5) it is possible to derive an equation relating  $\ln(t_n)$  and  $H$  for the strong domain wall pinning regime

$$\ln(t_n) = \frac{E_{\text{strong}}}{kT} \left[1 - \left(\frac{H}{H_0}\right)^{1/2}\right]^{3/2} - \ln(f_0). \quad (7)$$

The slope of Eq. (7) is

$$\frac{\Delta \ln(t_n)}{\Delta H} = \frac{-3E_{\text{strong}}}{4kTH_0} \left(\frac{H_0}{H} - \left(\frac{H_0}{H}\right)^{1/2}\right)^{1/2} \propto v_a \quad (8)$$

which is field dependent. It is important to note that Eq. (8) breaks down when  $H > H_0$ , therefore, Eq. (7) can only be compared with experiment at fields less than  $H_0$ .

### 3. Sample preparation and experiment

Two sputter deposited samples were studied, the preparation of which is described in detail elsewhere [10]. Sample A had the structure 24(14.3 Å Tb + 8.5 Å Fe) and sample B 18(19.8 Å Tb + 8.5 Å Fe). Both samples possessed glass substrates and were deposited without seed layers. A 90 Å protective layer of Al was deposited on top of the magnetic layers to prevent oxidation. Fig. 1 shows that both samples possessed hysteresis loops with very high squareness. The loops exhibit shearing, beginning at  $-0.5M_s$  and  $+0.35M_s$  for samples A and B, respectively. The shearing of the loops is typical of that observed for magneto-optic films exhibiting domain wall pinning [3] and indicates the fields at which such pinning occurs. Thus, at fields less than or equal to the coercivity, domain wall pinning is expected to be weak for sample A and strong for sample B. Sample A had a coercivity of 701 Oe and sample B a coercivity of 154 Oe.

Magnetic measurements were performed at room temperature using a commercial alternating gradient force magnetometer (AGFM)<sup>1</sup> possessing a very low-noise base of  $2 \times 10^{-8}$  emu, fast data acquisition time, high applied field sweep rate, small settling time, and field control to within 1 Oe [11]. In order to probe  $t_n$ , a series of what we term nucleation time experiments were performed on each sample. Each measurement consists of applying a saturating field to the sample, followed by a reversing field of appropriate value. The magnetic moment is then monitored until it drops by a predetermined amount, at least two orders of magnitude larger than the noise base of the AGFM (7.5% for sample A and 10% for sample B) and the elapsed time ( $t_n$ ) recorded. To obtain statistically valid sets of data these measurements were repeated 130 times for sample A and 500 times for sample B at each applied field. Applied fields less than the coercivity were used for sample A as it exhibited extremely rapid time dependence, while applied fields around the coercivity were used for sample B.

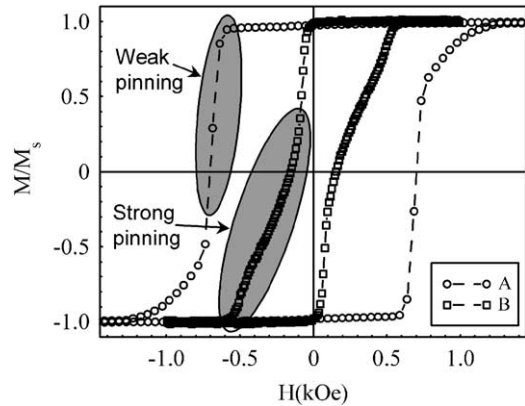


Fig. 1. Hysteresis loops for samples A and B. The shaded areas indicate where reversal is mainly by either reverse domain nucleation followed by weakly pinned domain wall motion or strongly pinned domain wall motion.

### 4. Results and discussion

A distribution in  $t_n$  over a range of the order of seconds was observed for both samples. Examples of the data are shown by the histograms in Figs. 2 and 3. For ease of interpretation the  $x$ -axis is plotted on a  $\log_e$  scale. The range is at least two orders of magnitude greater than the time resolution of the AGFM ( $\sim 10$  ms) and hence the distribution cannot be attributed to experimental uncertainties. The observed distributions are a result of the random nature of the thermal fluctuations responsible for time-dependent reversal. It is clear from Figs. 2 and 3 that modal values of  $t_n$  may be identified from the peak in the distributions, hence the variation of  $t_n$  with applied field may be probed.

Figs. 4 and 5 show the variation of  $t_n$  with applied field for samples A and B, respectively. For comparison with the theory,  $t_n$  is plotted on a  $\log_e$  scale. Fig. 4 reveals a linear relationship between  $\ln(t_n)$  and  $H$  for sample A. This is observed at applied fields where reversal is expected to proceed by reverse domain nucleation and rapid expansion due to weak domain wall pinning. The following function, which is of the form of Eq. (6) has been fitted to the experimental data and is indicated by the dashed line in Fig. 4:

$$\ln(t_n) = aH + b, \quad (9)$$

<sup>1</sup>Princeton Measurements Corporation "Micromag" 2900.

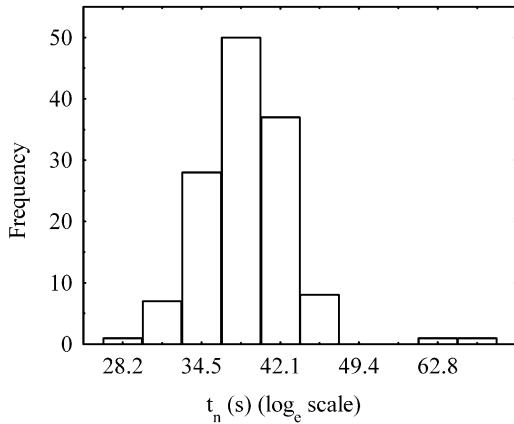


Fig. 2. Histogram of 130 nucleation time experiments performed on sample A at an applied field of  $-400$  Oe. The  $x$ -axis is plotted on a  $\log_e$  scale.

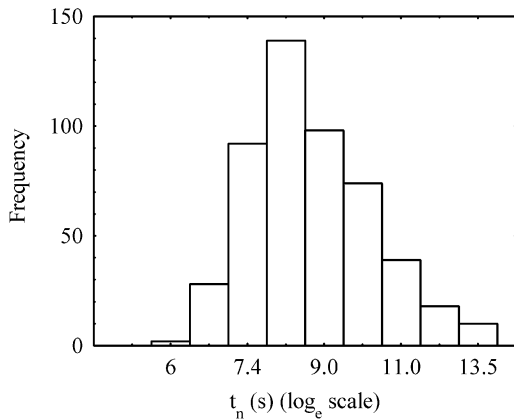


Fig. 3. Histogram of 500 nucleation time experiments performed on sample B at an applied field of  $-200$  Oe. The  $x$ -axis is plotted on a  $\log_e$  scale.

where  $a$  and  $b$  are fitting parameters. The fit of Eq. (9) to the experimental data is good. This implies that for this field range magnetisation reversal for sample A is described by the theoretical framework developed by Gaunt for the case of weak domain wall pinning [7,8].

A non-linear relationship is observed between  $\ln(t_n)$  and  $H$  for sample B with a minimum being observed at around  $-100$  Oe. Following the discussion of Eqs. (7) and (8) it is only appropriate to try to fit data to the right of the minimum, however, due to the small data set the point at

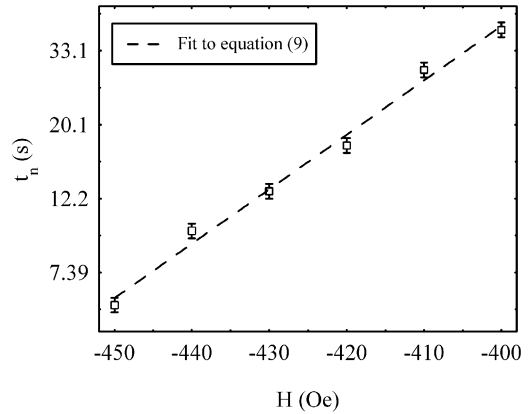


Fig. 4.  $\ln(t_n)$  vs.  $H$  for sample A, the  $y$ -axis is plotted on a  $\log_e$  scale for ease of interpretation. The dashed line is a least-squares fit of Eq. (9) to the experimental data and indicates that domain wall pinning is weak in the indicated field range for this sample.

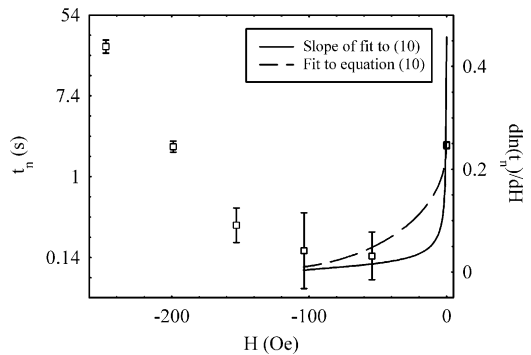


Fig. 5.  $\ln(t_n)$  vs.  $H$  for sample B, the  $y$ -axis is plotted on a  $\log_e$  scale for ease of interpretation. The dashed line is a fit of Eq. (10) to the experimental data, the solid line is the slope of the fitted curve.

$-104$  Oe has been included in the data to which the following curve has been fitted

$$\ln(t_n) = a \left[ 1 - \left( \frac{H}{b} \right)^{1/2} \right]^{3/2} + c, \quad (10)$$

where  $a$ ,  $b$  and  $c$  are fitting parameters. The fit of Eq. (10) to the experimental data is not good, although it does lie within the error bars. This indicates that magnetisation reversal may proceed in accordance with the Freidel steady-state model and that the theoretical framework of Gaunt is

probably applicable in this field range. It should be stressed that the evidence is not absolutely conclusive and that a larger set of experimental data would allow more accurate fitting and further clarification.

If it is assumed that the Freidel steady-state model is applicable between 0 and  $-100$  Oe, then the solid line in Fig. 5, corresponding to the slope of the fitted curve, indicates that the activation volume decreases as  $H_0$  is approached. This is due to the large demagnetising field associated with thin films possessing perpendicular magnetic anisotropy. Under such conditions the total field provides enough energy to either nucleate large domains, or nucleate small domains which are then able to expand via weak domain wall pinning energy barriers being overcome. In both cases, strong domain wall pinning prevents explosive expansion of the nucleated domains. As  $H_0$  is approached, the magnetisation and demagnetising field of the sample decreases. There is now insufficient energy to nucleate large domains or for energy barriers due to weak domain wall pinning to be overcome. Hence, the activation volume drops to a minimum.

## 5. Conclusion

The theoretical work of Gaunt addressing time dependence in systems possessing weak and strong domain wall pinning has been used to derive a linear relationship between  $\ln(t_n)$  and applied field, where  $t_n$  is the reverse domain nucleation time, for magneto-optic films exhibiting weak pinning. A non-linear relationship, applicable over a restricted field range, was derived for the strong domain wall pinning case. The results of reverse

domain nucleation time experiments performed on a Tb/Fe multilayer film exhibiting weak domain wall pinning have quantitatively confirmed the linear relationship. Experimental results for a sample exhibiting strong domain wall pinning provide initial confirmation of the validity of the relationship derived for strong pinning over a restricted range of applied fields.

## Acknowledgements

We thank Dr. T. Thomson for supplying the samples and Professor G. Bayreuther for allowing the use of his facilities for their preparation. This work was supported financially by the UK EPSRC.

## References

- [1] N. Sato, *J. Appl. Phys.* 59 (7) (1986) 2514.
- [2] M. Mansuripur, *Physical Principles of M-O Recording*, Cambridge University Press, Cambridge, 1995.
- [3] D.M. Donnet, V.G. Lewis, J.N. Chapman, K. O'Grady, H.W. van Kesteren, *J. Phys. D* 26 (1993) 1741.
- [4] M. El-Hilo, K. O'Grady, R.W. Chantrell, *J. Magn. Magn. Mater.* 109 (1992) L164.
- [5] M. El-Hilo, K. O'Grady, R.W. Chantrell, D.P.E. Dickson, *J. Magn. Magn. Mater.* 123 (1993) 30.
- [6] R. Street, S. Brown, *J. Appl. Phys.* 76 (10) (1994) 6386.
- [7] P. Gaunt, *J. Appl. Phys.* 59 (12) (1986) 4129.
- [8] P. Gaunt, *Philos. Mag. B* 48 (1983) 261.
- [9] S.D. Brown, R. Street, R.W. Chantrell, P.W. Haycock, K. O'Grady, *J. Appl. Phys.* 79 (5) (1996) 2594.
- [10] T. Thomson, K. O'Grady, G. Bayreuther, *J. Phys. D* 30 (1997) 1577.
- [11] K. O'Grady, V.G. Lewis, D.P.E. Dickson, *J. Appl. Phys.* 73 (10) (1993) 5608.